Cellular and Molecular Life Sciences (2025) 82:202
https://doi.org/10.1007/s00018-025-05698-6

ORIGINAL ARTICLE

GPI-anchorless prion disease is sensitive to oxidative stress and shows potential for treatment with edaravone, based on iPS-derived neuron study

Kosuke Matsuzono[1] · Hiroyuki Honda[2,3] · Takafumi Mashiko[1] · Reiji Koide[1] · Eiji Sakashita[4] · Hitoshi Endo[4] · Tetsuyuki Kitamoto[5] · Shigeru Fujimoto[1]

Received: 10 February 2025 / Revised: 27 March 2025 / Accepted: 4 April 2025

Abstract

Only a few reports have generated induced pluripotent stem cells from patients with prion diseases, making it important to conduct translational studies using cells derived from individuals with prion protein (*PRNP*) mutations. In this study, we established induced pluripotent stem cells from a patient with a glycosylphosphatidylinositol-anchorless *PRNP* mutation (Y162X), which leads to abnormal deposits of prion protein in various organs. While no abnormal intracellular prion protein deposits were observed in the neurons differentiated from *PRNP* Y162X induced pluripotent stem cells, extracellular PrP aggregates secretions were significantly increased, and these cells were significantly more sensitive to oxidative stress compared to control cells. Utilizing this *PRNP* Y162X iPSC-derived neuron model, we discovered that edaravone reduced the sensitivity of *PRNP* Y162X cells to oxidative stress. Following this finding, we treated a *PRNP* Y162X patient with edaravone for two years, which successfully suppressed indicators of disease progression. Our study demonstrates that the pathology of the glycosylphosphatidylinositol-anchorless *PRNP* mutation is associated with oxidative stress and highlights the potential of induced pluripotent stem cell technology in identifying novel treatments for rare prion diseases.

Keywords Edaravone · GPI anchor · iPSCs · Oxidative stress · Prion

Introduction

Prion diseases are rare progressive neurodegenerative conditions without effective treatment [1]. One of the reasons for this is that it has proven difficult to develop models of human prion diseases. We and Mead et al. independently reported that some *PRNP* truncation mutations can cause a noteworthy phenotype [2, 3] called "PrP systemic amyloidosis" [4], which is characterized by abnormal prion protein (PrP) deposits in whole organs. After these initial reports, different *PRNP* truncation mutations were identified that also cause PrP systemic amyloidosis [5–7].

The use of patient-derived induced pluripotent stem cells (iPSCs) to model neurological diseases is well-established [8, 9]. Patient-derived iPSC technology is considered valuable for modeling prion diseases that involve rare *PRNP* mutations. Here, we generated iPSCs from a patient with the *PRNP* Y162X mutation, which leads to PrP systemic amyloidosis [5, 10, 11], and differentiated them into neurons.

✉ Kosuke Matsuzono
kmatsuzono51@jichi.ac.jp

1 Division of Neurology, Department of Medicine, Jichi Medical University School of Medicine, Yakushiji 3311-1, Shimotsuke, Tochigi 329-0498, Japan

2 Department of Neuropathology, Graduate School of Medical Sciences, Kyushu University, Fukuoka, Japan

3 Neuropathology Center, Department of Neurology, National Hospital Organization, Omuta National Hospital, Fukuoka, Japan

4 Department of Biochemistry, Jichi Medical University, Tochigi, Japan

5 Division of CJD Science and Technology, Department of Neurological Science, Tohoku University Graduate School of Medicine, Miyagi, Japan

Published online: 15 May 2025

Finally, we applied our findings from the iPSC research to a clinical *PRNP* Y162X case for treatment.

Materials and methods

Full methodology for this study is described in the Supplemental manuscript.

Human subjects

This study was approved by the Ethics Committees of Jichi Medical University, Kyushu University, and Tohoku University, and it obtained approval from the Institutional Review Board (approval no.: Rin-Dai 22–165). Informed consent was obtained from all participants.

iPSC-derived neurons PrP analyses

We have developed human iPSCs and differentiated neuronal cells as described previously (Supplemental manuscript) [12–15]. We have performed immunocytochemistry, western blotting, and neurotoxicity assays in the presence of oxidative stress to this iPSC model.

After immunostaining of iPSCs and induced pluripotent stem cell-derived neurons (iPSNs), the cells were imaged using automated microscopy by an Operetta CLS (PerkinElmer) and then the immunostained structures were quantified automatically with an Operetta CLS High Content Analysis System (PerkinElmer). The signals, which fluoresced with Alexa-Fluor 488, 546, or DAPI, exceeding the scaffold were calculated as positive.

To analyze the secretion of extracellular PrP in the iPSNs model, we inserted collagen matrix gel into each iPSN culture during Days 31 to 50. We prepared the collagen matrix gel in a size of 1 cm x 1 cm x 0.5 cm using Cellmatrix Type I-A (Nitta Gelatin Connect and Create, Osaka, Japan), and placed it in the 6-well cultured iPSNs medium. After the gel was was collected and frozen using liquid nitrogen, it was cut into 20 µm sections with a cryostat (Leica Biosystems, Nussloch, Germany). These sections were immunostained with a mouse monoclonal anti-PrP antibody (3F4, Merck, MAB1562) and Alexa Fluor 546 fluoresce. Images were captured using a confocal laser microscope (Dragonfly 200, Oxford Instruments Andor Ltd, Belfast, Northern Ireland).

iPSC-derived neurons experiments to oxidative stress and Edaravone challenge test

For neurotoxicity assays in the presence of oxidative stress, iPSNs at Day 50 were treated with 0, 250, 500, 750, 1,000, or 2,000 µM H_2O_2 for 24 h. iPSN cell status at each H_2O_2 concentration was evaluated using cell viability, MAP-2-positive cell number, cell toxicity, reactive oxygen species (ROS) formation, and mitochondria fat-soluble peroxide.

iPSNs at Day 50 were treated with 1,000 µM H_2O_2 and 0, 25, 50, 75, or 100 µM edaravone (Tocris Bioscience, Bristol, UK) for 24 h. iPSN cell status at each edaravone concentration with 1,000 µM H_2O_2 was evaluated using cell viability, MAP-2-positive cell number, cell toxicity, ROS formation, and mitochondria fat-soluble peroxide.

Edaravone treatment of a *PRNP* Y162X patient

Based on the *in vitro PRNP* Y162X experimental results and permission from Jichi Medical University with informed consent from the patient, we treated a *PRNP* Y162X patient with edaravone. Edaravone treatment was initiated when the patient was 50s age and we compared the following parameters at 2 years before and at 2 years after edaravone treatment. The edaravone treatment protocol was based on its usage in patients with amyotrophic lateral sclerosis [16] with minor adjustments, which consisted of Cycle 1: 30 mg/day edaravone for 14 days and observation for 42 days; Cycle 2: 30 mg/day edaravone for 10 days and observation for 42 days; and the Cycle 2 protocol was repeated until the end of the study period.

Since the effect of the *PRNP* Y162X mutation is distributed throughout the autonomic system, multiple parameters were used to assess disease progression (Supplemental manuscript).

Statistical analysis

All in vitro experiments were performed using each iPSN clone plated in three wells. Three healthy iPSN clones and three *PRNP* Y162X iPSN clones were analyzed in all in vitro experiments, and values were calculated. Values are expressed as the mean ± standard error of the mean (SEM). Well-plate experiences and gained images by the Operetta CLS were quantified automatically. According to the extracellular PrP analyses obtained from the Dragonfly200, we captured fifteen section images of each cell clone and analyzed them using ImageJ. Significant differences among groups were determined by ANOVA. Differences were considered significant when $p < 0.05$, and calculations were performed with JMP 17 statistical software (SAS Institute, Inc., Cary, NC, USA).

Results

Generation of iPSC clones and neural differentiation

iPSC clones were generated from peripheral blood mononuclear cells of a healthy control and a *PRNP* Y162X patient (Table 1). All clones expressed the pluripotency markers in immunostaining (Fig. 1A) and were confirmed to retain genomic information (Fig. 1B). There was no obvious difference in neuronal differentiation propensity between control and *PRNP* Y162X clones (Fig. 1C and D).

No abnormal PrP deposits in *PRNP* Y162X iPSNs

We previously detected abnormal PrP deposits in *PRNP* Y162X patient tissue [10, 11], although the location of these abnormal PrP deposits was pathologically ambiguous. Thus, we first expected abnormal intracellular PrP deposits could occur in *PRNP* Y162X patient-derived iPSNs; however, there were no abnormal PrP deposits in these iPSNs, which were the same as those from the healthy control (Fig. 2A and B) at Day 50 and Day 72. Western blotting analysis also showed no abnormal PrP deposits in *PRNP* Y162X patient-derived iPSNs (Fig. 2C).

Extracellular secretion of aggregated PrP in *PRNP* Y162X iPSC-derived neurons

Contrary to the intracellular iPSNs results, extracellular secretions of aggregated PrP were significantly positive only in the *PRNP* Y162X patient-derived iPSNs (Fig. 2D). The co-culture collagen matrix gel showed PrP aggregation positive number/1-visual field as 20.2 ± 6.1 in *PRNP* Y162X vs. 4.6 ± 0.2 in healthy control ($p < 0.05$*) (Fig. 2E).

PRNP Y162X iPSC-derived neurons are sensitive to oxidative stress

According to our previous autopsy analysis [17] and previous reports on GPI-anchored PrP function [18], we suspected that the *PRNP* Y162X mutation increases sensitivity to oxidative stress. In order to examine our hypothesis, oxidative stress in iPSNs was assessed using five different parameters (Fig. 3). Cell viability decreased significantly more in *PRNP* Y162X iPSNs compared to healthy control iPSNs at H_2O_2 concentrations > 500 µM (Fig. 3B). The number of MAP-2-positive cells was also decreased significantly more in *PRNP* Y162X iPSNs than in healthy control iPSNs by H_2O_2-induced oxidative stress (Fig. 3A left and 3 C). Corresponding to cell viability, cell toxicity, as assessed using a lactate dehydrogenase assay, was significantly more elevated in *PRNP* Y162X iPSNs than in healthy control iPSNs at H_2O_2 concentrations > 250 µM (Fig. 3D). ROS were elevated significantly more in *PRNP* Y162X iPSNs than in healthy control iPSNs at 500 and 750 µM H_2O_2 (Fig. 3A middle and 3E). Mitochondrial fat-soluble peroxide was also elevated significantly more in *PRNP* Y162X iPSNs than in healthy control iPSNs at H_2O_2 concentrations > 750 µM (Fig. 3A right and 3 F).

Edaravone improves the sensitivity of *PRNP* Y162X iPSC-derived neurons to oxidative stress

Edaravone was considered as a potential drug to rescue *PRNP* Y162X pathology because it is the approved drug for the treatment of ischemic stroke [19] and amyotrophic lateral sclerosis [20] as a free radical scavenger. The effectiveness of edaravone was assessed first using the iPSN model.

As a result, edaravone showed effectiveness against oxidative stress in *PRNP* Y162X and healthy control iPSNs. In addition, edaravone was found to be more effective in *PRNP* Y162X iPSNs and it increased the response of *PRNP* Y162X iPSNs against oxidative stress closer to that of healthy control iPSNs. Edaravone at concentrations > 50 µM significantly improved cell viability in *PRNP* Y162X iPSNs (Fig. 4B). Edaravone also significantly increased the number of MAP-2-positive cells in both iPSN clones (Fig. 4A left and 4 C). Edaravone at concentrations > 75 µM significantly decreased cell toxicity only in *PRNP* Y162X iPSNs (Fig. 4D). In the presence of oxidative stress, edaravone concentrations > 25 µM significantly decreased ROS levels in *PRNP* Y162X iPSNs (Fig. 4A middle and 4E).

Table 1 List of induced pluripotent stem cell clones

Experimental clone	Clone name at establishment	Somatic cell	Sex	Donor age (years)	Reprogramming vector
Control					
Control-1	hc1-A	PBMC	female	65	episomal
Control-2	hc1-B	PBMC			episomal
Control-3	hc1-C	PBMC			episomal
***PRNP*Y162X**					
Y162X-1	Pri1-A	PBMC	female	57	episomal
Y162X-2	Pri1-B	PBMC			episomal
Y162X-3	Pri1-C	PBMC			episomal

PBMC, peripheral blood mononuclear cell

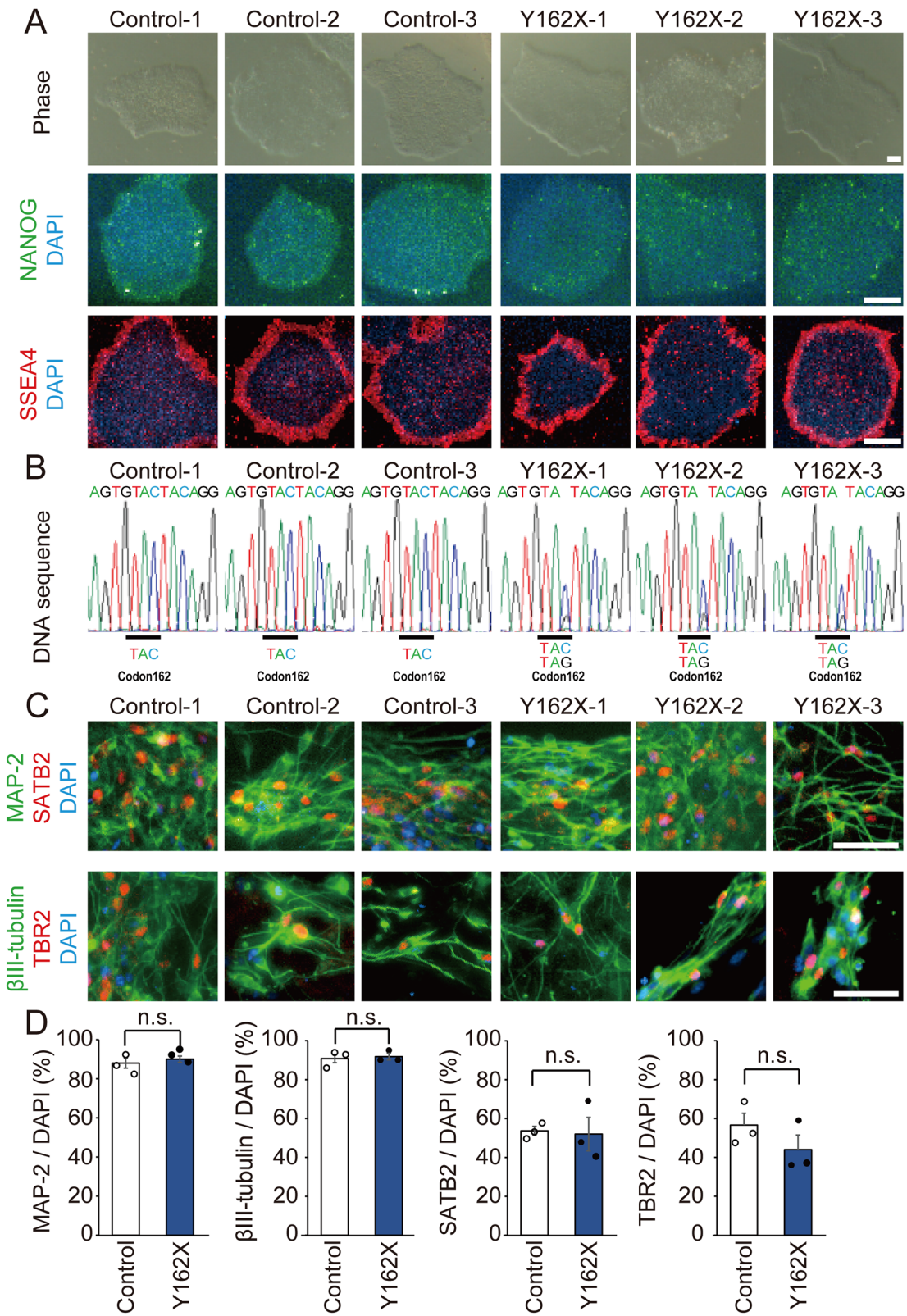

Mitochondrial fat-soluble peroxide was also significantly decreased by edaravone concentrations > 50 μM in *PRNP* Y162X iPSNs (Fig. 4A right and 4 F).

Clinical effects of edaravone on a *PRNP* Y162X patient

Fig. 1 Generation of iPSC clones and neural differentiation. (**A**) From each subject, three iPSC clones were generated. iPSCs from a healthy control and *PRNP* Y162X patient showing embryonic stem cell-like morphology (phase) and expressing pluripotent stem cell markers such as NANOG (green) and SSEA4 (red). Scale bars, 100 μm. (**B**) Sequences of the *PRNP* PCR products are shown. A single TAC allele at codon 162 is observed in healthy control clones, while TAC and TAG alleles at codon 162 are found in *PRNP* Y162X patient clones. (**C**) Differentiation of neural cells containing cortical neurons from iPSC clones. The generated neurons expressed the neuronal markers MAP-2 and ßIII-tubulin, and cortical neuron markers SATB2 and TBR2. Scale bars, 50 mm. (**D**) There were no significant differences in the differentiation propensity of neurons or cortical neurons between healthy control and *PRNP* Y162X patient iPSC clones. Values are expressed as the mean ± SEM from $n = 3$ clones. n.s., not significant

On the basis of the results in *PRNP* Y162X iPSNs, we considered that edaravone was a potential treatment for *PRNP* Y162X patients. We treated a *PRNP* Y162X patient with edaravone for 2 years and compared several pathological parameters between before and after treatment. The clinical results are shown in Table 2; Fig. 5. The patient maintained her nutritional status solely through oral intake of normal food, and no routine parenteral or enteral nutrition was introduced through this study period. As a result, most of the parameters were improved or maintained after edaravone treatment. According to physical status, the body mass index was approximately maintained and the Barthel Index was improved after edaravone treatment. Cognitive function worsened before edaravone treatment, but improved after treatment. Blood examinations of nutritional status also worsened before edaravone treatment, but improved after treatment. Both arterial blood gas analysis and the apnea hypopnea index showed an improvement after treatment.Through continued edaravone treatment, the patient still survives and maintains the activities of daily living by oneself at home.

Discussion

In this study, we established iPSC clones from a patient with a *PRNP* mutation Y162X. Although we found no intracellular PrP deposits, we discovered that *PRNP* Y162X iPSNs were significantly more sensitive to oxidative stress. Using in vitro iPSN model and demonstrating that edaravone reduced the sensitivity of *PRNP* Y162X iPSNs to oxidative stress, we treated the *PRNP* Y162X patient with edaravone, which helped suppress the patient's clinical symptoms.

After 2020, several studies involving iPSCs focusing on prion diseases have been reported [21–25]. Some studies established *PRNP* E200K iPSCs [21–24], while others investigated *PRNP* Y218N [25]. Our study is the first iPSC study of the nonsense-type *PRNP* mutation associated with GPI-anchorless prion disease, PrP systemic amyloidosis [4].

As well as the other *PRNP* mutations [21–25], our *PRNP* Y162X iPSC results showed no intracellular PrP deposits. The reason why there were no intracellular PrP deposits in this study remains unclear, but some factors can be considered. One possibility is that an abnormal intracellular PrP formation using iPSC model is extremely challenging because abnormal PrP formation progresses slowly and requires a long period of time while the iPSCs may be too immature [26]. The other possibility is that there is no intracellular deposition but only extracellular PrP secretion in PrP systemic amyloidosis. Previous reports support this hypothesis, as PrP without a GPI anchor has the characteristic of not localizing at cell membrane surface but being released into the culture [27, 28], while some PrP without a GPI anchor can be degraded rapidly by the proteasome-mediated pathway [29].

According to the oxidative sensitive of *PRNP* Y162X, some speculations can be considered. One is the influence of physiological GPI-anchor function. The GPI anchor is essential for the protective effect of PrPc against oxidative stress [18], and there is a possibility that the result from the GPI-anchorless mutation of codon 162 is involved with oxidative stress sensitivity. The second is the influence on the PrPc dynamics because the PrPc has complex dynamics; cleavage, secretion, and recycling [30].

Additional discussions including limitations of this study are detailed in the Supplemental manuscript.

In conclusion, we generated iPSCs and differentiated neurons from a GPI-anchorless *PRNP*-mutated patient. *PRNP* Y162X iPSNs were sensitive to oxidative stress, but edaravone partially rescued this sensitivity. Finally, we succeeded in treating and maintaining a clinical *PRNP* Y162X patient for at least 2 years with edaravone.

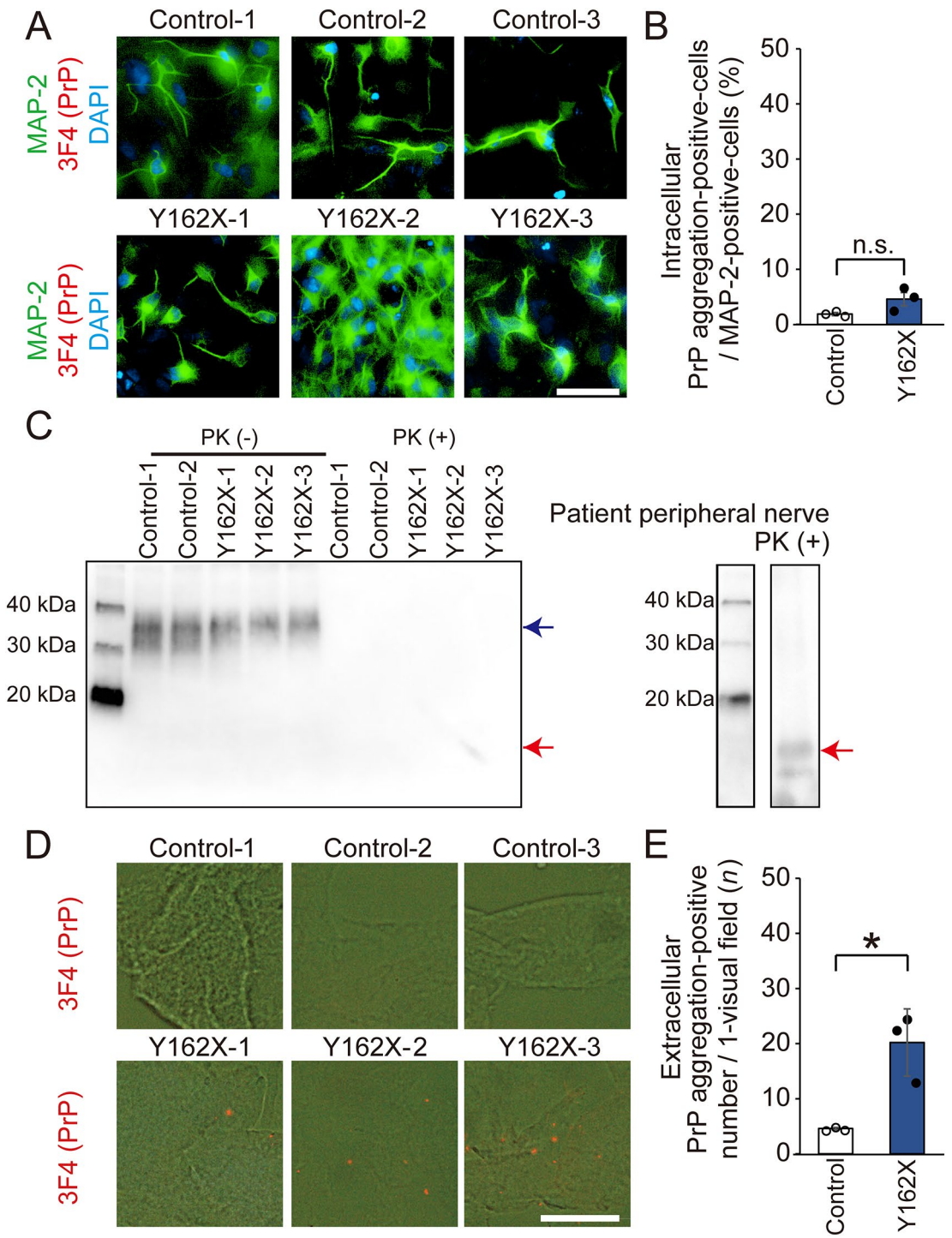

Fig. 2 Abnormal PrP deposit analysis in *PRNP* Y162X iPSNs. Immunocytochemistry analysis (**A**, **B**) revealed no abnormal intracellular deposits of prion protein (PrP) in both *PRNP* Y162X iPSNs and healthy control iPSNs. The positive PrP staining was quantified automatically. Scale bars represent 50 µm. Data are presented as the mean ± SEM from a total of 3 clones, with n.s. indicating not significant results. Western blot analysis (**C**) also indicated that no abnormal PrP deposits were formed. Following proteinase K treatment, all proteins were digested, and no protein bands were detected in either the healthy control or the *PRNP* Y162X iPSNs (left panel), in contrast to the positive control derived from a patient's left sural nerve (right panel). The blue arrow points to the PrPc band, while the red arrow indicates the abnormal PrPres band observed in *PRNP* GPI-anchorless disease. (**D**, **E**) Extracellular PrP aggregations absorbed to collagen matorix gel. Scale bars represent 50 µm. Contrary to the intracellular results, the PrP aggregations detected by anti-PrP antibody were only present in *PRNP* Y162X iPSNs

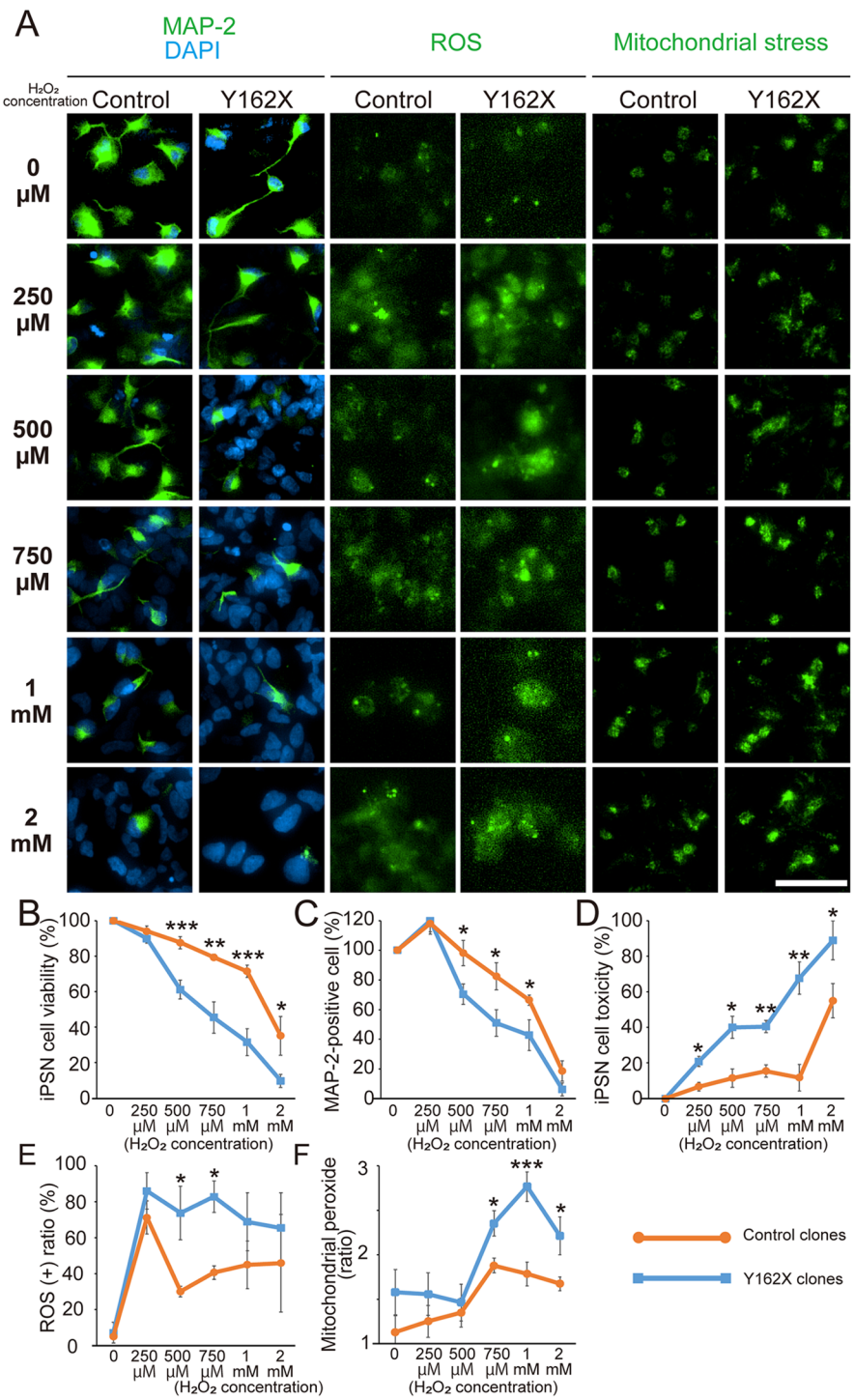

Fig. 3 Sensitivity of *PRNP* Y162X iPSNs to oxidative stress. (**A**) Fluorescence images of immunochemistry, ROS, and mitochondrial fat-soluble peroxide in healthy control and *PRNP* Y162X patient iPSNs at H_2O_2 concentrations of 0, 250, 500, 750, 1,000, and 2,000 µM. Scale bars, 50 mm. Comparison of (**B**) cell viability, (**C**) number of MAP-2-positive cells, (**D**) cell toxicity, (**E**) ROS response ratio, and (**F**) mitochondrial peroxide levels between healthy control and *PRNP* Y162X patient iPSNs. The comparison was performed between clone types (healthy control and *PRNP* Y162X) at each H_2O_2 concentration. *$p<0.05$, **$p<0.01$, and ***$p<0.001$. Data are presented as the mean ± SEM from $n=3$ clones

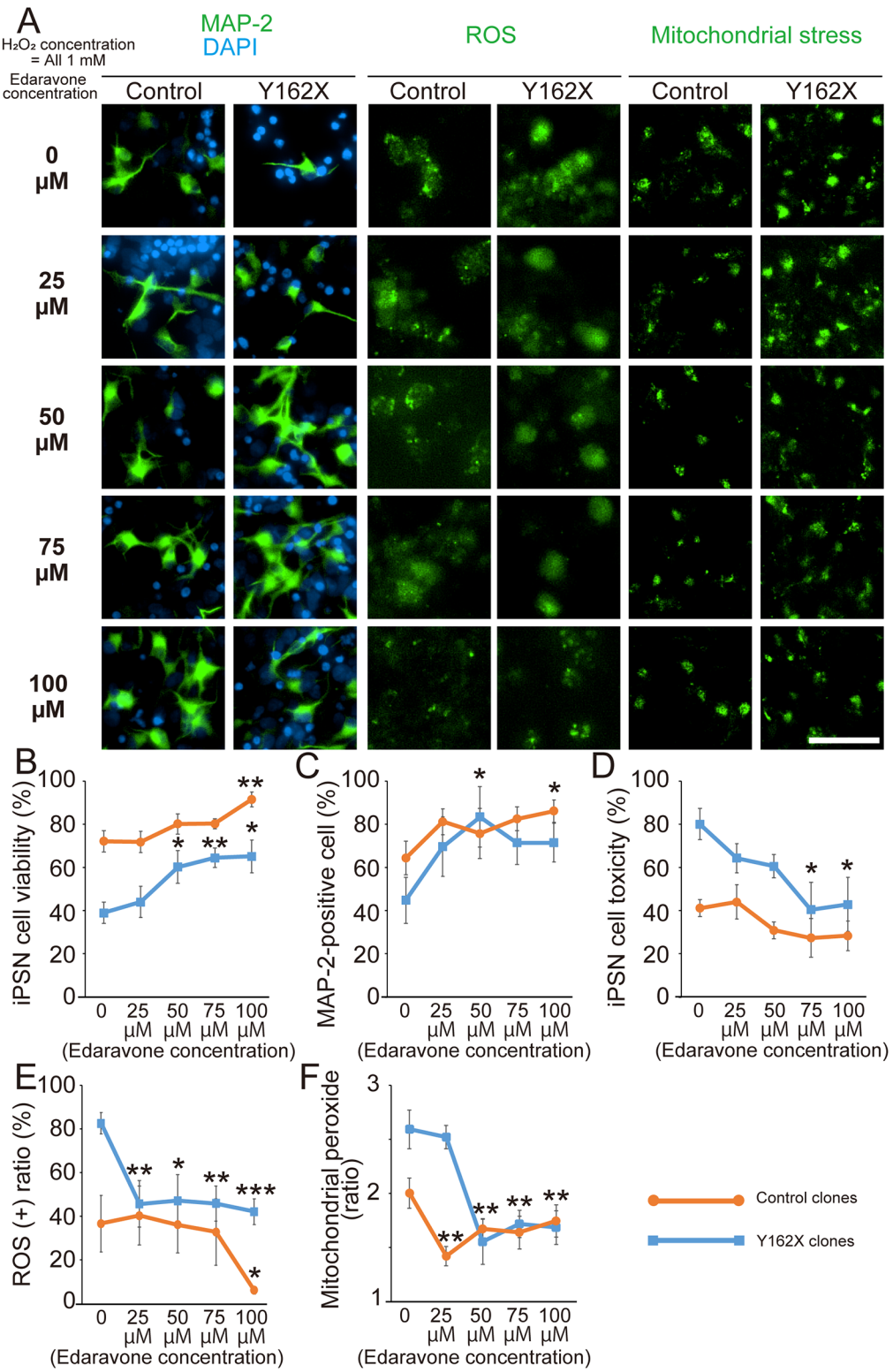

Fig. 4 Effect of edaravone on the sensitivity of *PRNP* Y162X iPSNs to oxidative stress. (**A**) Fluorescence images of immunochemistry, ROS, and mitochondrial fat-soluble peroxide in healthy control and *PRNP* Y162X patient iPSNs with 1,000 μM H_2O_2 at 0, 25, 50, 75, and 100 μM edaravone. Scale bars, 50 mm. Comparison of (**B**) cell viability, (**C**) number of MAP-2-positive cells, (**D**) cell toxicity, (**E**) ROS response ratio, and (**F**) mitochondrial peroxide levels among edaravone concentrations in healthy control and *PRNP* Y162X patient iPSNs. The comparison was performed between 0 μM edaravone and each edaravone concentration. *$p<0.05$, **$p<0.01$, and ***$p<0.001$. Data are presented as the mean ± SEM from $n=3$ clones

Table 2 Comparison of the disease parameters before and after edaravone treatment in the *PRNP* Y162X patient

	Edaravone treatment (-)			Edaravone treatment (+)		Parameter change	
	2 years before edaravone initiation	1 year before edaravone initiation	Edaravone initiation	1 year after edaravone initiation	2 years after edaravone initiation	Edaravone (-) 2 years	Edaravone (+) 2 years
Physical status							
BMI	18.7	18.2	17.5	17.6	17.4	-1.2	-0.1
Barthel Index	100/100	95/100	85/100	95/100	100/100	-15	+15
Cognitive function							
MMSE	30/30	26/30	29/30	30/30	30/30	-1	+1
MoCA	25/30	23/30	22/30	25/30	25/30	-3	+3
Blood exam							
Alb (g/dL)	3.6	3.7	3.3	3.6	3.7	-0.3	+0.4
Pre-Alb (mg/dL)	20.0	21.4	18.1	20.4	23.2	-1.9	+5.1
Transferrin (mg/dL)	333	273	248	248	313	-85	+65
ABG							
$PaCO_2$ (mmHg)	45.7	42.8	47.2	41.2	44.0	+1.5	-3.2
PaO_2 (mmHg)	79.4	70.3	86.1	83.8	94.8	+6.7	+8.7
NCS							
Sural SNAP potential	(+)	(+)	(+)	(+)	(+)	-	-
Median F wave appearance (%)	75	56	62	68	87	-13	+15
Physiological exam							
ABPM							
Maximum BP CV (%)	20.2	-	20.7	-	16.5	+0.5	-4.2
Mean BP CV (%)	20.0	-	24.9	-	16.5	+4.9	-8.4
Minimum BP CV (%)	21.6	-	28.9	-	17.8	+7.3	-11.1
Polysomnography							
AHI	11.2	-	21.3	-	16.0	+10.1	-5.3
[^{123}I]MIBG scintigraphy							
H/M early ratio	1.97	-	2.28	-	2.14	+0.31	-0.14
H/M late ratio	1.63	-	1.70	-	2.00	+0.07	+0.30
Heart washout rate (%)	29.9	-	34.1	-	30.7	+4.2	-3.4

In parameter change, blue items show improvement and red ones worsening. ABG: air blood gas; ABPM: ambulatory blood pressure monitoring; AHI: apnea hypopnea index; Alb: albumin; BMI: body mass index; BP: blood pressure; CV: coefficient of variation; H/M: heart/mediastinum; [^{123}I]MIBG: iodine-131-labeled metaiodo-benzylguanidine; MMSE: Mini-Mental State Examination; MoCA: Montreal Cognitive Assessment; NCS: nerve conduction study; SNAP: sensory nerve action potential

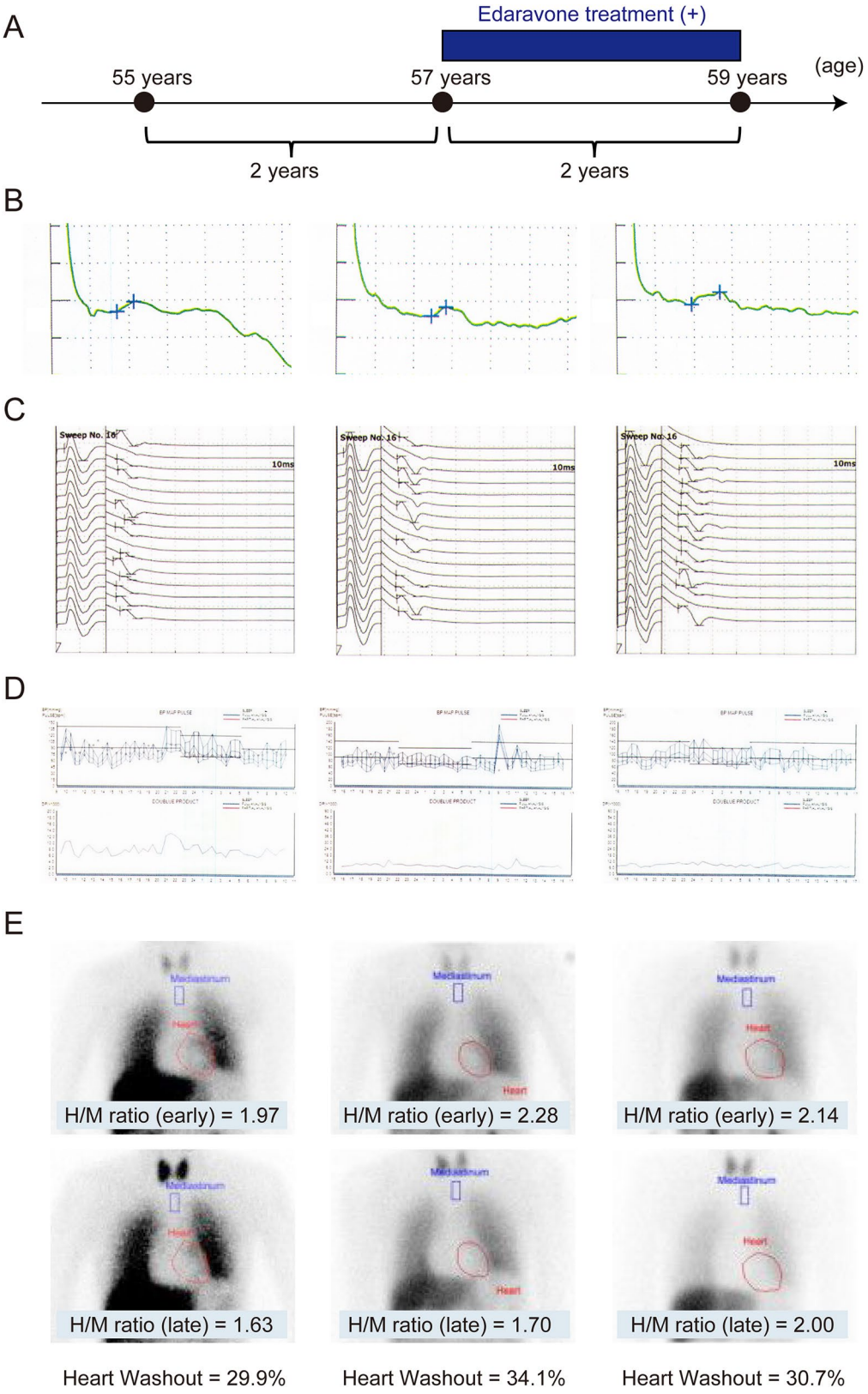
A
Edaravone treatment (+)
55 years
57 years
59 years
(age)
2 years
2 years
B
C
Sweep No. 16
10ms
D
E
H/M ratio (early) = 1.97
H/M ratio (early) = 2.28
H/M ratio (early) = 2.14
H/M ratio (late) = 1.63
H/M ratio (late) = 1.70
H/M ratio (late) = 2.00
Heart Washout = 29.9%
Heart Washout = 34.1%
Heart Washout = 30.7%

Fig. 5 Clinical effect of edaravone on a *PRNP* Y162X patient. (**A**) Edaravone treatment protocol for the *PRNP* Y162X patient. (**B**) Nerve conduction study showing the preservation of the compound sensory action potential of the sural nerve throughout the study period. (**C**) The appearance rate of the median F wave improved after edaravone treatment, which changed from 75% at 2 years before to 62% at edaravone initiation and 87% at 2 years after. (**D**) Ambulatory blood pressure monitoring showing the fluctuation of blood pressure was reduced after edaravone treatment. (**E**) Changes of the iodine-131-labeled metaiodo-benzylguanidine (^{131}I-MIBG) scintigraphy results, heart to mediastinum (H/M) ratio and heart washout rate, are shown. Heart washout rate, as assessed by ^{131}I-MIBG scintigraphy, which reflects sympathetic function, worsened before edaravone treatment, but improved after treatment

Supplementary Information The online version contains supplementary material available at https://doi.org/10.1007/s00018-025-05698-6.

Acknowledgements We would like to express our sincere gratitude to all our coworkers and collaborators; Akemi Makino, Yuhei Anan, Masayuki Suzuki, Miyu Usui, Risa Suzuki, Shyuya Hirano, Kazumasa Sekiguchi, Chie Ueki, Akito Mori, Kazuhiro Saito, and Ayaka Kakurai. We appreciate REPROCELL Inc. for generating iPSCs. We are grateful to the YOKOYAMA Foundation for Clinical Pharmacology and the Ministry of Education, Science, Culture, and Sports of Japan for providing grants-in-aid for this study.

Author contributions K.M. conceived the project. K.M., H.H., H.E., and T.K. designed the experiments. K.M., H.H., and E.S. performed the experiments. K.M. and H.H. analyzed the data. K.M., T.M., and R.K. were the attending doctors of the presented case. K.M. and S.F. wrote the manuscript. S.F. supervised the project. All authors read and approved the final manuscript.

Funding This work was partly supported by a grant from the YOKOYAMA Foundation for Clinical Pharmacology (YRY-2002) and a Grant-in-Aid for Scientific Research (Early-Career) 21K15231 from the Ministry of Education, Science, Culture, and Sports of Japan.

Data availability All experiment raw data included in this study have been deposited and opened in Mendeley Data (DOI; https://doi.org/10.17632/n8wzg53f7p.1). All data according to this study are available from the corresponding authors on request.

Declarations

Ethics approval and consent to participate This study was approved by the Ethics Committees of Jichi Medical University, Kyushu University, and Tohoku University, and it obtained approval from the Institutional Review Board (approval no.: Rin-Dai 22–165). Informed consent was obtained from all participants.

Consent for publication All authors consented to publish the manuscript.

Conflict of interest The authors declare no competing interests.

References

1. Stewart LA, Rydzewska LH, Keogh GF et al (2008) Systematic review of therapeutic interventions in human prion disease. Neurology 70:1272–1281
2. Mead S, Gandhi S, Beck J et al (2013) A novel prion disease associated with diarrhea and autonomic neuropathy. N Engl J Med 369:1904–1914
3. Matsuzono K, Ikeda Y, Liu W et al (2013) A novel Familial prion disease causing pan-autonomic-sensory neuropathy and cognitive impairment. Eur J Neurol 20:e67–69
4. Mead S, Reilly MM (2015) A new prion disease: relationship with central and peripheral amyloidoses. Nat Rev Neurol 11:90–97
5. Bommarito G, Cellerino M, Prada V et al (2018) A novel prion protein gene-truncating mutation causing autonomic neuropathy and diarrhea. Eur J Neurol 25:e91–92
6. Fong JC, Rojas JC, Bang J et al (2017) Genetic prion disease caused by PRNP Q160X mutation presenting with an orbitofrontal syndrome, Cyclic diarrhea, and peripheral neuropathy. J Alzheimers Dis 55:249–258
7. Capellari S, Baiardi S, Rinaldi R et al (2018) Two novel PRNP truncating mutations broaden the spectrum of prion amyloidosis. Ann Clin Transl Neurol 5:777–783
8. Egawa N, Kitaoka S, Tsukita K et al (2012) Drug screening for ALS using patient-specific induced pluripotent stem cells. Sci Transl Med 4:145ra04
9. Matsuzono K, Imamura K, Murakami N et al (2017) Antisense oligonucleotides reduce RNA foci in spinocerebellar Ataxia 36 patient iPSCs. Mol Ther Nucleic Acids 8:211–219
10. Matsuzono K, Kim Y, Honda H et al (2021) Prion gene PRNP Y162X Truncation mutation can induce a refractory esophageal achalasia. Am J Gastroenterol 116:1350–1351
11. Matsuzono K, Kim Y, Honda H et al (2021) Optic nerve atrophy and visual disturbance following PRNP Y162X Truncation mutation. J Neurol Sci 428:117614
12. Poleganov MA, Eminli S, Beissert T et al (2015) Efficient reprogramming of human fibroblasts and Blood-Derived endothelial progenitor cells using nonmodified RNA for reprogramming and immune evasion. Hum Gene Ther 26:751–766
13. Nakagawa M, Taniguchi Y, Senda S et al (2014) A novel efficient feeder-free culture system for the derivation of human induced pluripotent stem cells. Sci Rep 4:3594
14. Kondo T, Asai M, Tsukita K et al (2013) Modeling Alzheimer's disease with iPSCs reveals stress phenotypes associated with intracellular Abeta and differential drug responsiveness. Cell Stem Cell 12:487–496
15. Morizane A, Doi D, Kikuchi T et al (2011) Small-molecule inhibitors of bone morphogenic protein and activin/nodal signals promote highly efficient neural induction from human pluripotent stem cells. J Neurosci Res 89:117–126
16. Writing G, Edaravone ALSSG (2017) Safety and efficacy of Edaravone in well defined patients with amyotrophic lateral sclerosis: a randomised, double-blind, placebo-controlled trial. Lancet Neurol 16:505–512

17. Matsuzono K, Honda H, Sato K et al (2016) PrP systemic deposition disease': clinical and pathological characteristics of novel Familial prion disease with 2-bp deletion in codon 178. Eur J Neurol 23:196–200
18. Foliaki ST, Wood A, Williams K et al (2023) Temporary alteration of neuronal network communication is a protective response to redox imbalance that requires GPI-anchored prion protein. Redox Biol 63:102733
19. Feng S, Yang Q, Liu M et al (2011) Edaravone for acute ischaemic stroke. Cochrane Database Syst Rev. CD007230
20. Rothstein JD (2017) Edaravone: A new drug approved for ALS. Cell 171:725
21. Foliaki ST, Groveman BR, Yuan J et al (2020) Pathogenic prion protein isoforms are not present in cerebral organoids generated from asymptomatic donors carrying the E200K mutation associated with Familial prion disease. Pathogens 9:482
22. Wood AR, Foliaki ST, Groveman BR et al (2022) Hereditary E200K mutation within the prion protein gene alters human iPSC derived cardiomyocyte function. Sci Rep 12:15788
23. Smith A, Groveman BR, Winkler C et al (2022) Stress and viral insults do not trigger E200K PrP conversion in human cerebral organoids. PLoS ONE 17:e0277051
24. Gojanovich AD, Le NTT, Mercer RCC et al (2024) Abnormal synaptic architecture in iPSC-derived neurons from a multi-generational family with genetic Creutzfeldt-Jakob disease. Stem Cell Rep 19:1474–1488
25. Matamoros-Angles A, Gayosso LM, Richaud-Patin Y et al (2018) iPS cell cultures from a Gerstmann-Straussler-Scheinker patient with the Y218N PRNP mutation recapitulate Tau pathology. Mol Neurobiol 55:3033–3048
26. Medvedev SP, Shevchenko AI, Zakian SM (2010) Induced pluripotent stem cells: problems and advantages when applying them in regenerative medicine. Acta Naturae 2:18–28
27. Campana V, Caputo A, Sarnataro D et al (2007) Characterization of the properties and trafficking of an anchorless form of the prion protein. J Biol Chem 282:22747–22756
28. Shen P, Dang J, Wang Z et al (2021) Characterization of anchorless human PrP with Q227X stop mutation linked to Gerstmann-Sträussler-Scheinker syndrome in vivo and in vitro. Mol Neurobiol 58:21–33
29. Zanusso G, Petersen RB, Jin T et al (1999) Proteasomal degradation and N-terminal protease resistance of the codon 145 mutant prion protein. J Biol Chem 274:23396–23404
30. Harris DA (2003) Trafficking, turnover and membrane topology of PrP. Br Med Bull 66:71–85